Angular distributions and rotational excitations for electron scattering from ozone molecules

F. A. Gianturco* and P. Paioletti
Department of Chemistry, The University of Rome, Cittá Universitaria, 00185 Rome, Italy

N. Sanna
Center for Supercomputing Applications to Scientific Research, Cittá Universitaria, 00185 Rome, Italy
(Received 21 January 1998; revised manuscript received 11 June 1998)

Ab initio quantum scattering calculations are carried out for the O_3 molecule, in its ground electronic state, from which low-energy electrons are scattered in the gas phase. The results of the computations are compared with the existing experimental angular distributions for elastic (rotationally summed) scattering processes and for rotationally inelastic cross sections. The agreement of the present calculations with the available experiments is found to be remarkably good and the corresponding efficiency of rotationally inelastic processes is also discussed and analyzed in terms of the role played by the small permanent dipole moment of this target molecule. [S1050-2947(98)01211-6]

PACS number(s): 34.80.Bm

I. INTRODUCTION

Ozone is one of the most important gases in the Earth's atmosphere and is probably the substance most commonly associated with atmospheric chemistry. As we have been told many times, ozone's presence in the upper atmosphere is essential to all forms of life as it screens out for us the deadly part of the UV radiation. Once down in the troposphere, on the other hand, ozone becomes a pollutant since not only is it toxic to both plants and animals but it turns out to also be corrosive to most materials [1,2]. It therefore becomes increasingly more useful to acquire as much information as possible on the chemical and physical properties both of the ozone molecule itself and of its interactions with other molecules and elementary partners.

Having information on the general features of the scattering of electrons by ozone is especially important to the studies of upper atmosphere processes, where the electronic quenching mechanisms and energy transfer efficiency involving O_3 lower-lying electronic states can increase the populations of its excited states, thereby perturbing the local thermodynamic equilibrium. The consequences of such changes in local population can then appear as increased emission from infrared-active gases, thereby affecting radiative cooling and the temperature structure of the atmosphere [2]. On the other hand, perhaps because of its difficult preparation and handling and its corrosive properties, fairly few experimental studies have been carried out on this system. Electron-energy-loss spectra (EELS) of ozone have been reported by Celotta, Mielczarek, and Kuygatt [3] and Swanson and Celotta [4]. Further energy-loss spectra and absolute differential cross sections (DCSs) were also reported at energies between 3 and 20 eV and angles between 12° and 168° [5]. More recently, an experimental collaboration between University College and Oxford [6,7] reported vibrational energy-loss spectra along a series of energies between 3.5 and 7.0 eV, over a range of scattering angle between 40° and 120°. Mason *et al.* [8] further reported low-energy EELS data using an electron trap arrangement. Partial electron ionization cross sections for incident electron energies from 40 to 500 eV have also been determined by using time-of-flight mass spectrometry [9], while, most recently, the dissociative electron attachment in ozone has been explored first for electron energies between 0 and 10 eV [10] and later on by Skalny *et al.* [11] and by Allan *et al.* [12], who also reported vibrationally inelastic differential cross sections in the resonance region.

The corresponding theoretical studies on the structure of ozone in its ground electronic state and in its lower-lying electronic states have also been quite extensive over the years, as could be gleaned from the discussion and results of Ref. [13]. On the other hand, the actual calculations for the scattering dynamics and scattering observables in the case of electron as projectiles have been rather few and fairly limited in scope: High-energy scattering ($E_{\mathrm{coll}} \geqslant 300$ eV) was discussed earlier on by using a model potential [14] and total cross sections at slightly lower energies were also computed using a model optical potential [15]. No calculations, however, had appeared at a more sophisticated level before the work of Okamoto and Itikawa [16], in which differential, integral, and momentum transfer cross sections were computed for the vibrationally elastic process at collision energies between 5 and 20 eV. Further *ab initio* work at the exact static-exchange (ESE) level of approximation was carried out more recently by Sarpal *et al.* [17] using the polyatomic *R*-matrix method, where integral elastic scattering cross sections were evaluated and compared with the few existing experiments. Additional static-exchange calculations have been recently completed by making use of the Schwinger variational iterative method (SVIM) [18] and they will be also compared below with the present results.

In the present work we decided to carry out *ab initio*, nonempirical calculations that also include correlation-polarization effects via a model local potential (see below) and that further add corrections necessary to deal with a polar target within the fixed nuclei (FN) frame of reference, as

*Author to whom correspondence should be addressed. FAX: +39-6-49913305. Electronic address: FAGIANT@CASPUR.IT

we shall show in detail later on. We also make use of the single-center (SC) expansion method and solve the corresponding close-coupled (CC) equations in the body-fixed (BF) reference. Additionally we have evaluated rotationally inelastic, partial state-to-state cross sections and have analyzed the corresponding efficiency of that specific energy transfer process. The paper is organized as follows. In Sec. II we outline the present theoretical treatment. In Sec. III we compare the present calculations with the available experiments and with other theoretical results. In Sec. IV we discuss the behavior of the rotationally inelastic collisions. The final conclusions are briefly summarized in Sec. V.

II. THEORETICAL TREATMENT

A. Scattering equations

We describe the collisional process in terms of the solutions of the Schrödinger equation (in a.u.) in the form

$$H\psi(\mathbf{r},\mathbf{X}) = E\psi(\mathbf{r},\mathbf{X}), \tag{1}$$

where

$$H = \hat{T} + \hat{V} + \hat{H}_{\mathrm{mol}} \tag{2}$$

and $\hat{T}$ is the kinetic energy of the incident electron, $\hat{V}$ is its interaction with the molecular nuclei and electrons

$$\hat{V} = \sum_{i=1}^{N} |\mathbf{r}-\mathbf{x}|^{-1} + \sum_{\gamma=1}^{M} \mathbf{Z}_\gamma |\mathbf{r}-\mathbf{X}_\gamma|^{-1}, \tag{3}$$

$\hat{H}_{\mathrm{mol}}$ is the Hamiltonian for the molecular target, and $\mathbf{r}$ is the position of the continuum electron. We let $\mathbf{X}$ represent collectively the coordinates of the target electrons $\mathbf{x}_i$ $(i=1,N)$ and the molecular nuclei $\mathbf{X}_\gamma$ $(\gamma=1,M)$. We also intend to refer all particles to a frame of reference fixed to the molecule (the BF frame). The molecular Hamiltonian $\hat{H}_{\mathrm{mol}}$ describes not only the interaction among the electrons and nuclei but also their respective motion. One now converts the many-body problem to an effective single-particle one by expanding the total system wave function ψ in terms of a complete set of target states as

$$\psi(\mathbf{r},\mathbf{X}) = \sum_{\alpha} \hat{\mathbf{A}}\{\mathbf{F}_\alpha(\mathbf{r})\phi_\alpha(\mathbf{X})\} \tag{4}$$

such that

$$\hat{H}_{\mathrm{mol}}\phi_\alpha(\mathbf{X}) = \epsilon_\alpha\phi_\alpha(\mathbf{X}), \tag{5}$$

where $\hat{A}$ is the antisymmetrization operator and ϵ_α are the molecular eigenvalues for each asymptotic (isolated) molecular electronic (n) and rotovibrational $(J\tau v)$ state of the target $\alpha \equiv |n_\alpha J_\alpha \tau_\alpha v_\alpha\rangle$. Here J and τ represent the two quantum numbers for the asymmetric rotor target [19], while v stands collectively for the vibrational quantum numbers of the three molecular normal modes. Now inserting Eq. (5) into Eq. (1) and multiplying on the left by the conjugate of a representative state of Eq. (4), one obtains the familiar set of coupled integro-differential equations

$$H_\alpha F_\alpha(\mathbf{r}) = \sum_\beta \mathbf{Z}_{\alpha\beta}(\mathbf{r}), \tag{6}$$

which constitute the general CC equations of the scattering problem, with the following meaning of symbols:

$$H_\alpha = [\nabla + k_\alpha], \tag{7}$$

$$Z_{\alpha\beta}(\mathbf{r}) = \int \mathbf{K}_{\alpha\beta}(\mathbf{r}|\mathbf{r}_1)\mathbf{dr}_1, \tag{8}$$

$$K_{\alpha\beta}(\mathbf{r}|\mathbf{r}_1) = \mathbf{V}_{\alpha\beta}(\mathbf{r}_1)\,\delta(\mathbf{r}-\mathbf{r}_1) + \mathbf{W}_{\alpha\beta}(\mathbf{r}|\mathbf{r}_1). \tag{9}$$

Here k_α^2 is given by $2(E-\epsilon_\alpha)$. The direct electrostatic interaction $V_{\alpha\beta}$ is local and is given by an integral, involving the interaction $\hat{V}$ of Eq. (2) and two target states $\langle\alpha|\hat{V}|\beta\rangle$. The nonlocal exchange interaction is represented schematically by $W_{\alpha\beta}$, a complicated nonlocal term that will be discussed below. One finally extracts all the necessary collisional information, such as the reactance K, transition T, or scattering S matrices, from which the actual cross sections are determined, by matching the solutions F_α to their proper asymptotic forms. A final transformation to a space-fixed (SF) frame of reference finally provides the desired scattering observables that can be compared with the experimental findings.

The simplest *ab initio* treatment of Eq. (6) is to evaluate the direct and nonlocal interactions of Eqs. (7) and (8) without any further polarization effects. This is the so-called exact static-exchange level, whereby the target wave function ψ_0 is treated as a single Slater determinant for the ground state $|\alpha\rangle$ and the continuum functions that are solutions of Eq. (6) are generated numerically within the undistorted field of the fixed molecular nuclei and the ψ_0 electrons.

The further addition of short-range correlation effects between the bound and the continuum electrons, together with the long-range part of the polarization forces, could be found via the choice of a nonlocal, energy-dependent complex optical potential $V_{\mathrm{opt}}(\mathbf{r})$. However, we have introduced earlier in [20] a simpler formulation that employs the average correlation energy of a single particle, within the formalism of the Kohn-Sham variational theorem, to obtain the short-range correlation forces as an analytic function of the target electronic density $\rho_{HF}(\mathbf{r}_i)$. Such an analytic function can then be matched, in the long-range region, to the second-order perturbation expansion for the polarization potential

$$V_{\mathrm{pol}}^{(2)}(r) \approx -\sum_{l=1}^{\infty} \frac{\alpha_l}{2r^{2l+2}}, \tag{10}$$

where it is usually sufficient to employ the first multipolar coefficient, the target static dipole polarizability α_D. The final result will therefore provide us with a model correlation-polarization potential in the local form $V_{\mathrm{CP}}(\mathbf{r})$ [21]. One can thus construct the full interaction ESE potential by summing the contributions of the static, exchange, and V_{CP} potentials discussed above. Before doing that, however, we have represented all such potential terms, together with the bound molecular orbitals (MOs) and the total target electronic density, in a BF frame of reference centered in the

center of mass of the target molecule, thus following a single-center expansion (SCE) treatment of the CC scattering equations [21].

The calculation of the nonlocal exchange interaction requires the evaluation of the sum of integrals

$$\sum_{\eta} \int \phi_{\eta}^{*}(r')|r-r'|^{-1}F^{(p\mu)}(r')dr'\,\phi_{\eta}(r), \qquad (11)$$

where η sums over the occupied target MOs, given by the ϕ_{η} functions, and the $F^{(p\mu)}$ are the continuum electron functions for any irreducible representation (IR) labeled by the $|p\mu\rangle$ indices [19]. The corresponding matrix formulation of the CC equations (6) can be written as

$$LF_{i}^{(p\mu)} = WF_{i-1}^{(p\mu)}, \qquad (12)$$

where $WF_{i-1}^{(p\mu)}$ is the exchange term given by some initial estimate for $i=1$, $F_{0}^{(p\mu)}$, and the iterative procedure consists in generating the successive $F_{i}^{(p\mu)}$ matrices until convergence is achieved by the unchanged structure of the scattering K matrix within a given threshold of invariance for its matrix elements.

In practice, one rewrites the scattering equations in terms of the Lippmann-Schwinger equation for the scattering by a potential that is the difference between the local exchange potential and the exact exchange potential

$$\psi_{p} = \phi_{p} + G_{\alpha}V_{e}\psi_{p}, \qquad (13)$$

where ϕ_{p} is a solution to the purely local potential problem

$$H_{\alpha}\phi_{p} = E\phi_{p}. \qquad (14)$$

The local Hamiltonian H_{α} is $\frac{1}{2}\nabla^{2}+V_{\alpha}$, where V_{α} is the sum of the local potentials

$$V_{\alpha} = V_{\text{static}} + V_{\text{pol}} + V_{\text{model exchange}}. \qquad (15)$$

The potential V_{e} is defined by

$$V_{e} = V_{\text{exact exchange}} - V_{\text{model exchange}} \qquad (16)$$

and the Green's function is defined by

$$(E-H_{\alpha})G_{\alpha} = 1. \qquad (17)$$

If we define the total K matrix by

$$K_{pq} = K_{pq}^{(\alpha)} + K_{pq}^{(e)}, \qquad (18)$$

where $K^{(\alpha)}$ is the K matrix due to scattering only by V_{α}, then $K^{(e)}$ can be obtained as

$$K_{pq}^{(e)} = 2\langle \phi_{p}|V_{e}|\psi_{q}\rangle. \qquad (19)$$

B. Differential cross sections

We are considering here the scattering of an electron from a nonlinear molecule in the FN approximation. In the case of a polar molecule the partial-wave expansion of the differential cross section does not converge when evaluated in the fixed-nuclei approximation [20] and therefore an alternative procedure to circumvent this problem is employed in the present work.

The DCS is given by the familiar expression [19]

$$q = \sum_{L} A_{L}(\kappa^{2})P_{L}(\cos\,\theta), \qquad (20)$$

where P_{L} is the Legendre function. The A_{L} coefficients have already been given many times before (see, e.g., Ref. [19]) and therefore will not be repeated here. The T matrix is in turn defined as

$$T_{l'v'}^{lv} = \delta_{ll'}\delta_{vv'} - S_{l'v'}^{lv}, \qquad (21)$$

and the corresponding integral cross section is given by

$$Q = (\pi/k^{2})\sum_{l,v}\sum_{l',v'}|T_{l'v'}^{lv}|^{2}. \qquad (22)$$

It should be noted that the present cross sections q and Q correspond to the vibrationally elastic ones (i.e., summed over the final rotational states). In the fixed-nuclei approximation, those cross sections are independent of the initial rotational state [19–21].

If no approximations are made with respect to the rotovibrational molecular degrees of freedom involved in the dynamics and all calculations are carried out in the laboratory frame, SF frame of reference (for a recent review of the terminology see Ref. [19]), then the partial, state-to-state differential cross section for scattering into the polar angle ϑ can be expressed as a Legendre expansion with coefficients depending on the rotational quantum numbers of the asymmetric rotor

$$\frac{d\sigma}{d\Omega}(j\tau\rightarrow j'\tau') = k'/k\sum_{\lambda} A_{\lambda}(j\tau\rightarrow j'\tau')P_{\lambda}(\cos\,\vartheta), \qquad (23)$$

where the A_{λ} coefficients depend explicitly only on products of the elements of the transition matrix $\hat{T}$ and other algebraic factors [22,23]. Also $k'^{2} = k^{2} + 2(E_{j\tau} - E_{j'\tau'})$. Since their precise form involves in principle infinite sums over the angular momenta (ℓ,ℓ') characterizing the matrix elements of $\hat{T}$, then the presence of a very-long-range potential in the case of electron scattering from polar molecules implies that a very large number of A_{λ} coefficients need to be evaluated and therefore that a very large set of (ℓ,ℓ') indices of the $\hat{T}$ matrix need to be included in the exact calculations owing to the very slow convergence of the sum in Eq. (23).

When further simplifying the calculations by returning to the FN approximation in the BF frame of reference, the usual partial-wave expansion can be employed. However, in the case of polar molecules, the partial-wave expansion of the cross section does not converge if the fixed-nuclei approximation is applied as it stands. To remedy this difficulty, one can use the following closure formula instead [22–24]:

$$\frac{d\sigma}{d\Omega} = q^{B} + \sum_{L} (A_{L} - A_{L}^{B})P_{L}(\cos\,\theta). \qquad (24)$$

Here the superscript B denotes that the relevant quantity is calculated in the Born approximation with an electron-point-dipole interaction. The summation over L in Eq. (24) converges rapidly because the contribution from the higher partial waves to the DCS is dominated by the electron-dipole interaction and can be calculated in the Born approximation. The first term in Eq. (24) is then given via the formula

$$q^B=\sum_{j',\tau'} q^B_{\rm rot}(j\tau\rightarrow j'\tau'). \tag{25}$$

Here $(j\tau)$ denotes the rotational state of H_2O and $q^B_{\rm rot}(j\tau\rightarrow j'\tau')$ is the Born DCS for the rotational transition $j\tau\rightarrow j'\tau'$ calculated with a point-dipole interaction from a rotor scatterer. This has in turn the form [25]

$$q^B_{\rm rot}(j\tau\rightarrow j'\tau')=\frac{4}{3}\frac{k'}{k}(2j'+1)\mu^2|\langle j'\tau'|j\tau\rangle_{100}|^2 \times(k^2+k'^2-2kk'\cos\theta)^{-1}, \tag{26}$$

where k and k' are the wave numbers of the incident and the scattered electrons and $\mu^2|\langle j'\tau'|k\tau\rangle_{100}|^2$ is the squared dipole transition moment. The inelastic cross sections are calculated similarly by writing

$$Q=Q^B+4\pi(A_0-A_0^B), \tag{27}$$

with

$$Q^B=\sum_{j',\tau'} Q^B_{\rm rot}(j\tau\rightarrow j'\tau'), \tag{28}$$

and the Born cross section is given as

$$Q^B_{\rm rot}(j\tau\rightarrow j'\tau')=\frac{8\pi}{3}(2j'+1)\mu^2|\langle j'\tau'|j\tau\rangle_{100}|^2 \times\frac{1}{k^2}\ln\left|\frac{k+k'}{k-k'}\right|. \tag{29}$$

It should be noted that q^B and Q^B depend on the initial rotational state $(j\tau)$ and hence q and Q do also. The above formulas can be regarded as a correction to the Born approximation treatment of dipole interaction since they include short-range effects from the CC calculations. Clark [26] already discussed this point in the case of diatomic molecules.

One can rewrite Eq. (5) in a completely equivalent form [25]

$$\frac{d\sigma}{d\Omega}(vj\rightarrow v'j')=\frac{d\sigma^{\rm FBA}}{d\Omega}(vj\rightarrow v'j')+\Delta\frac{d\sigma}{d\Omega}(vj\rightarrow v'j'), \tag{30}$$

where

$$\Delta\frac{d\sigma}{d\Omega}(vj\rightarrow v'j')=\frac{1}{4k_{vj}^2}\sum_{\lambda}\{A_\lambda(vj\rightarrow v'j') -A_\lambda^{\rm FBA}(vj\rightarrow v'j')\}P_\lambda(\cos\vartheta). \tag{31}$$

Aided by cancellation, the sum over λ in Eq. (30) can now converge more rapidly and terminate for a given $\lambda_{\max}$ at a preselected accuracy. Thus the first term on the right-hand side of Eq. (30) represents the result from the use of the analytic Born expression, while the correction term of Eq. (30) first contains the contribution from the CC results and then subtracts from it a further term that is extracted from the unitarized Born formulation for the T matrix, as constructed from the first Born approximation K-matrix elements [27–29]. One should also note that a BF formulation of the adiabatic nuclear rotation approximation was used earlier on [27,28] to provide an entirely equivalent set of correction formulas that go under the name of mean approximation for the divergent DCS problem in polar diatomic targets. One should also note that an additional difficulty may appear when using Eq. (31) if the actual value of the dipole moment provided by the static interaction for the self-consistent-field target turns our to be much larger than the correct asymptotic dipole used in the last term of Eq. (31), hence causing the final DCS to become negative at some angles. In all our calculations, however, this disagreement did not occur and therefore all computed DCSs of Eq. (30) remained always positive. The final rotovibrationally (or only rotationally) inelastic cross section can then be written as

$$\frac{d\sigma^{\rm mean}}{d\Omega}(vj\rightarrow v'j')=\frac{d\sigma^{\rm FBA}}{d\Omega}(vj\rightarrow v'j') +\Delta\frac{d\sigma^{\rm mean}}{d\Omega}(vj\rightarrow v'j'). \tag{32}$$

III. COMPARISON WITH EXPERIMENTS

The ground-state electronic structure of ozone is given by the $^1A_1$ total symmetry. We carried out our calculations using a triple-ζ-plus-polarization quality of expansion over Gaussian-type orbitals labeled $(D95^{**}6d10f)$ obtained using the GAUSSIAN 94 suite of codes [30]. The equilibrium bond length and bond angle values were kept, within the FN approximation scheme, at $2.415a_0$ and at 116.8°, respectively. The corresponding total energy turned out to be $-224.049\,36$ hartree and the computed dipole moment values was -0.30 a.u., to be compared with the experimental value of -0.21 a.u. [31]. The value of the spherical polarizability employed to evaluate the $V_{\rm CP}$ correlation-polarization potential was $18.9a_0^3$. The single-center expansion was carried out at the center of mass of the system, which was located clearly off the positions of all three nuclear charges. The number of points was 300 for r, 48 for ϑ, and 21 for ϕ, making up a total of 302 400 evaluated points. The multipolar expansion of the static potential was carried out for both the electronic and nuclear parts, up to a $\lambda_{\max}$ value of 36, while the partial-wave expansion for the scattering electron was tested for a series of l values up to 18 with convergence achieved already for an $l_{\max}$ value of 12. The latter choice implied a total number of coupled equations in the A_1 symmetry of 100.

A. Question of the shape resonances

One of the issues that has been raised in relation to the behavior of the elastic cross sections in the low-energy regimes is that of the possible existence of broad shape reso-

nances in one or more of the symmetry channels. The experimental observations of several investigations [6,5,8–10,12] point to the presence of some broad shape resonances in the vibrationally inelastic channels only, whereby the extra electron is captured in very strongly antibonding σ^* orbitals, which are in turn modified by the bond stretching effects [12]. Thus the earlier findings were of two broad resonances peaking around 4.2 and 6.6 eV, assigned to totally symmetric vibrations of A_1 symmetry and to the antisymmetric stretch of B_2 symmetry. Further and more recent [32] experiments on the elastic integral cross sections between 0 and 10 eV have also confirmed the absence of similar shape features in the elastic channels scattering.

The earliest calculations that used a close-coupling approach that included a model polarization potential [16] did not show any indication of shape resonances in their computed elastic (rotationally summed) integral cross sections and their integral cross section (ICS) values appear to be flat over the whole energy range of relevance. They, however, gave results only on a sparse energy grid.

The *R*-matrix calculations of ICSs and momentum transfer cross sections (MTCSs) carried out at the static-exchange (SE) level [17], on the other hand, suggested the presence of various broad shape resonances in the elastic channels: two of A_1 symmetry at 8.2 eV and 18.0 eV, with widths of 2.6 and 0.8 eV, respectively, and two B_2 resonances at 11.1 and 18.1 eV, with widths of 2.0 and 0.8 eV, respectively. A further A_2 resonance around 20 eV was also suggested by them. A more recent and fairly extensive calculation at the SE level without inclusion of polarization effects has been carried out by Lee *et al.* [18]. These authors have analyzed the elastic ICSs and MTCSs over a more dense grid of energy values and found marked disagreement with the earlier *R*-matrix calculations: There are no signs of resonance in either the 8-eV or the (18–20)-eV ranges of energy, an indication of a weak and broad A_1 shape resonance around 11 eV and another possible broad and weak shape resonance of B_2 nature around 14 eV. They attributed this discrepancy to the truncation of the *R*-matrix calculations to the $l_c=3$ partial wave, which was too low since their calculations found instead that at least $l_c=8$ was needed to have converged cross sections to about 2%.

In our present analysis of the angular distributions and of the rotationally inelastic processes discussed below, we have also carried out a preliminary analysis of the A_1 component of the elastic ICS around the (6–8)-eV range over a more dense energy grid and found, as in Ref. [18], no indication of any shape resonance in that energy region. One should note here that we used l_c values up to 18 in some convergence tests and found that, in analogy with Ref. [18], l_c values up to 12 were needed for convergence around 1–2 %. Therefore, we have not further analyzed with a more dense grid of energy points the region around 10–16 eV where the SE shape resonances were seen by the recent calculations [18] since the experimentalists still insist on indicating that the possible shape resonances could be seen in the inelastic channels only. The current situation about shape resonances can therefore be summarized as follows: (i) The experimental data have seen the presence of shape resonance structures in the A_1 and B_2 symmetries, but only when the vibrationally inelastic channels are measured, with no indication

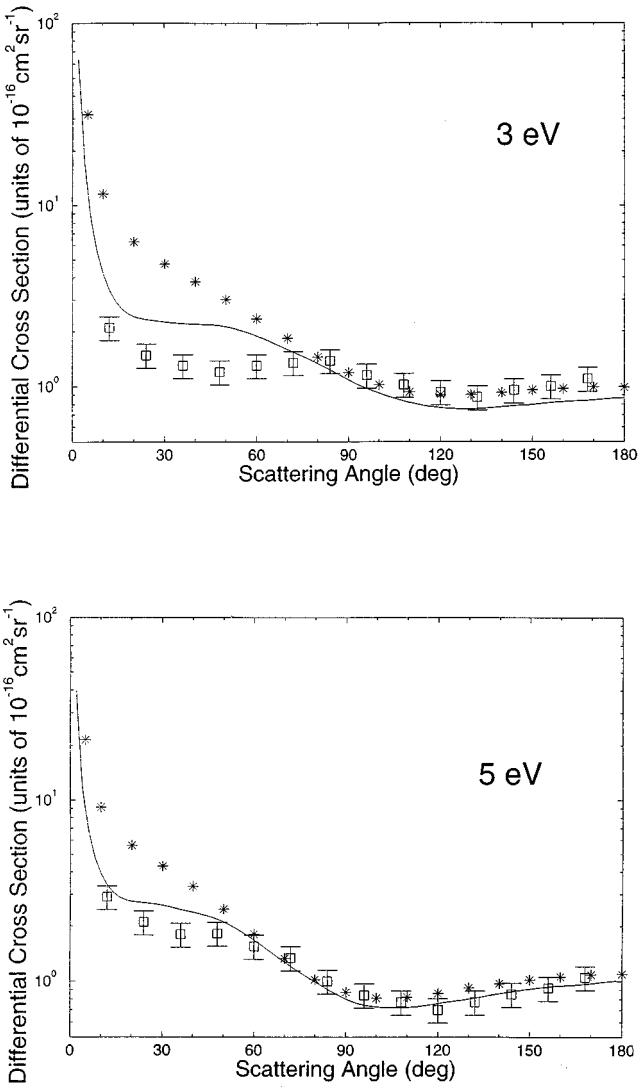

FIG. 1. Computed and measured elastic (rotationally summed) differential cross sections. The top diagram refers to 3.0 eV of collision energy, while the bottom diagram reports results at 5.0 eV. The open squares are the experiments from Ref. [5], while the present results are given by the solid line. The SVIM calculations of Ref. [18] are given by the sequence of asterisks.

of structures in the elastic cross sections [33]; (ii) the earlier computational suggestion of a possible A_1 shape resonance around 8 eV at the SE treatment of the elastic channel [17] has not been confirmed by the later calculations [18] nor by our present search of it in that symmetry; and (iii) the possible presence of two weak shape resonances of A_1 and B_2 symmetries in the elastic channels has been suggested by only one set of calculations [18] and, at the static-exchange level, in the (11–14)-eV energy range.

Since the present study has focused on the angular distributions and rotational excitation processes, we have decided to carry out elsewhere [34] a more detailed analysis of the higher-energy range where one set of calculations [18] suggests the existence of weak shape resonances, in order to see if their disagreement with the experiments could be attributed to any specific feature of the computational methods currently employed. The use of FN calculations, in fact, is known to magnify the ''bumps'' associated with shape reso-

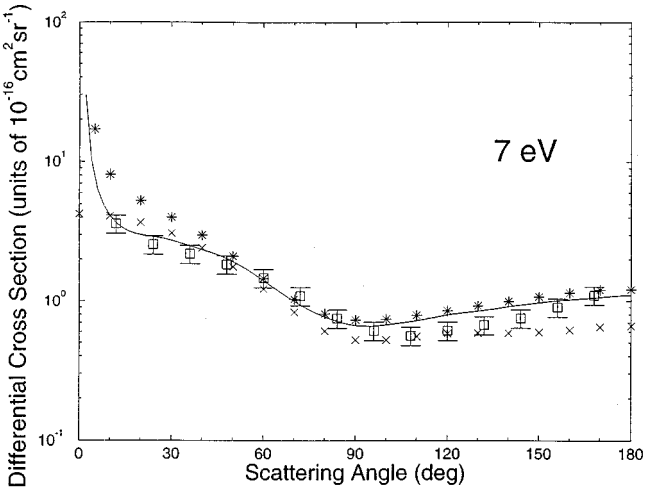

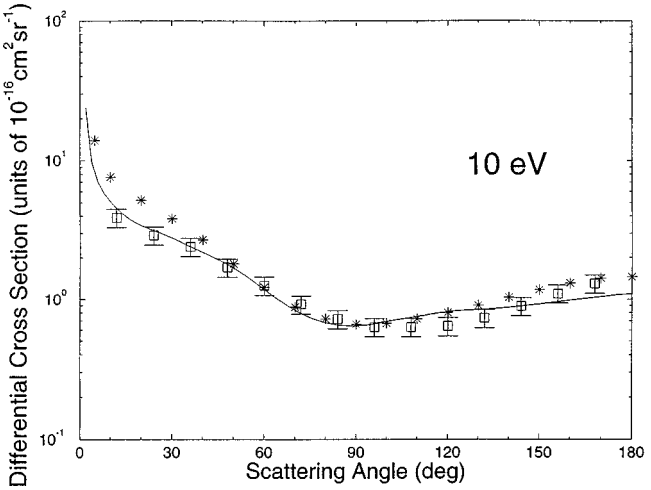

FIG. 2. Computed and measured elastic, rotationally summed, differential cross sections at 7.0 eV (top) and 10.0 eV (bottom) of collision energy. The notation is the same as in Fig. 1. The additional crosses are the pseudopotential calculations of Ref. [36].

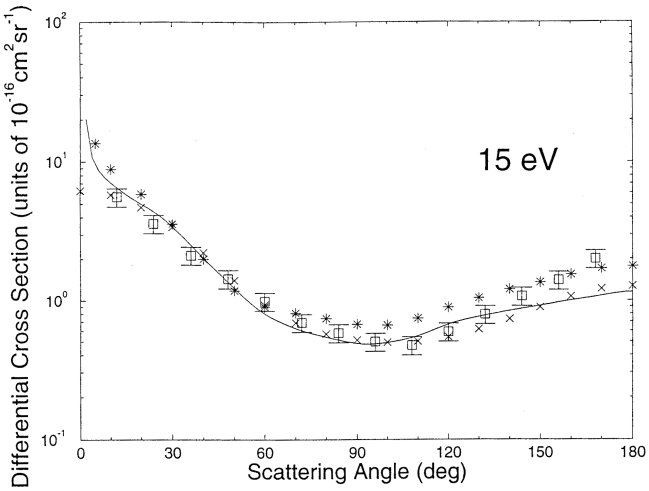

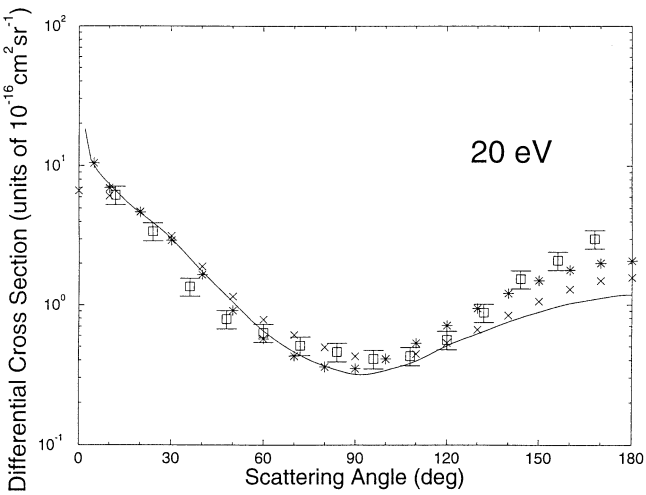

FIG. 3. Same as in Figs. 1 and 2, but for two higher collision energy values of 15.0 eV (top) and 20.0 eV (bottom). The notation is the same as in Figs. 1 and 2.

nances as the latter are usually lowered and broadened when nuclear motion is included [33] and therefore could be one of the possible causes of the lack of observation of such features in the measurements of the elastic integral cross sections in the (0–10)-eV range of energy [32].

B. Differential cross sections

As mentioned before, the detailed comparison of calculations with experimentally obtained angular distributions is a more direct test of the quality of a theoretical treatment for electron scattering from polar molecules [35]. The results reported in Fig. 1 for two different collision energies (3 and 5 eV) therefore show our computed elastic (rotationally summed) differential cross sections, which include the Born correction as outlined in Sec. II B and given by Eq. (24). In the upper part (at 3.0 eV) our calculated values (solid line) are compared with the experimental points (open squares) from Ref. [5] and with the ESE calculations of Ref. [18] (asterisks). One sees clearly that the agreement of our data with experiments is generally fair as the computed values follow closely the experimental points and further show the strong forward peak caused by the dipole scattering in the narrow angular cone below $\vartheta_{\text{c.m.}} \sim 10°$. The similar calculations at the ESE level are close to our results from $\sim 60°$ but are much larger in the small-angle region. The results at 5 eV, reported in the lower part of Fig. 1, show remarkable agreement between the present theory and the measured values. We also show in that part of the figure the recent calculations from the ESE variational approach of Ref. [18], given by the line of asterisks, and see that their agreement is only qualitatively acceptable below 50°, while following very closely our results in the larger-angle scattering.

If we now move to the higher collision energies reported in Fig. 2 and corresponding to 7.0 and 10.0 eV, respectively, we see that the agreement between the present theory and the experiments becomes really remarkable: Our computed values now remain within the experimental error bars at all the available angles and for both the energy values shown. As before, the asterisks also show the data at both energies from the ESE calculations of Ref. [18] and indicate once more a

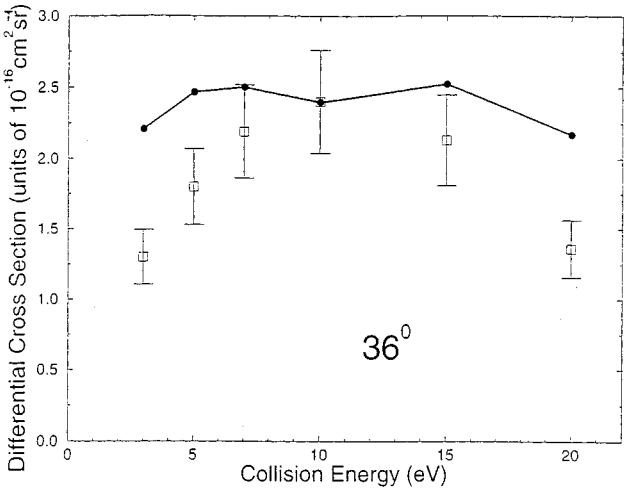

FIG. 4. Computed and measured energy dependence of the DCS at two different angles: 36° (top) and 96° (bottom). The experiments (open squares) are from Ref. [12]. The present calculations are the filled circles. The dotted line reports calculations from Ref. [17].

less satisfactory accord with the measured data. Additional recent calculations that employ the Schwinger multichannel method with pseudopotentials [36] are also shown by crosses for the collision energy of 7.0 eV: They agree well with our results at all angles, but have no forward peak. We show in Fig. 3 a comparison between the present and the Schwinger-type calculations of Refs. [18] and [36] at the higher collision energies of 15.0 and 20.0 eV, respectively. We see that all calculations are qualitatively very similar, although differences exist especially in the large-angle region where the different approaches employed to obtain the short-range interactions by the three theoretical methods clearly play a relevant role. On the whole, however, one can say that the calculated values for the DCS are shown to be in very good agreement with the available experiments and provide a reliable description of the e^--ozone scattering dynamics at low collision energies and for the vibrationally elastic channels.

A further interesting comparison of experimental data with calculations is shown in Fig. 4. We show there the

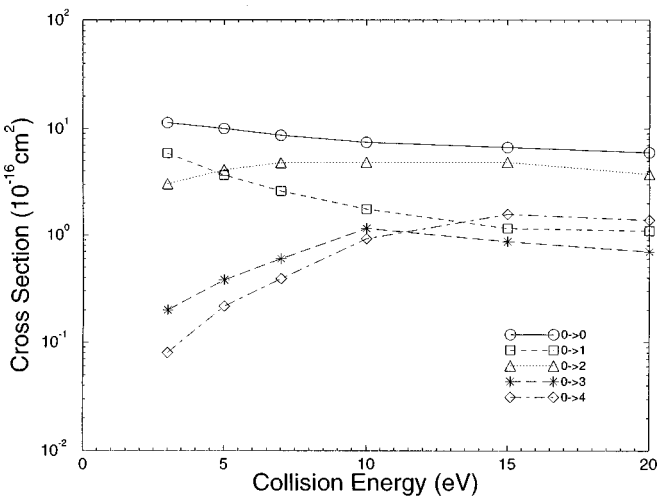

FIG. 5. Computed partial, state-to-state, integral cross sections as a function of collision energy. The symbols are explained in the figure itself.

energy dependence of the DCS at two different scattering angles: 36° (upper diagram) and 96° (lower diagram). The experimental data are from the measurements of the Friburg group [12] and the solid lines are the present calculations. At the larger angles we also report the *R*-matrix ESE calculations of Ref. [17] as a dotted curve. We clearly see once more that the present calculations follow the experimental behavior very closely within the energy range sampled by us and certainly agree with measurements better than the dotted curve data.

Because of the relatively low energies that can be exchanged in upper atmosphere processes or in the astrophysical environment of interest for ozone reactions it is still of interest, however, to obtain reliable information on the mechanisms involved and the values of the relative probabilities for collisional excitations of rotational levels of the ozone target at low collision energies. This aspect of the dynamics will be discussed in the following section.

IV. ROTATIONAL EXCITATION PROCESSES

The ozone molecule, like other C_{2v} systems such as H_2S, SO_2, and H_2O, is an asymmetric top rotor with three different rotational constants of 3.50, 0.44, and 0.39 cm^{-1}, respectively. This means that the energy transfer processes can involve transitions between $|J\tau\rangle$ states, where J is the principal quantum number and τ is a pseudoquantum number introduced to distinguish the $2J+1$ sublevels for a given J since the projection of the latter angular momentum along the BF axis is no longer a good quantum number. However, by summing over the final τ' allowed values for each transition and averaging over initial τ values, in the following discussion we will primarily consider $J \rightarrow J'$ transitions as being the basic energy transfer transitions over the same range of collision energy discussed earlier for the elastic cross sections. One should also note that, given the values of the three moments of inertia for this molecule, the possible amounts of energy that can be transferred in low $\Delta|J\tau\rangle$ transitions must of necessity be rather small. The calculations shown in Fig. 5 report the partial integral state-to-state cross sections, elastic and inelastic, from the initial $J=0$ level. Because of the

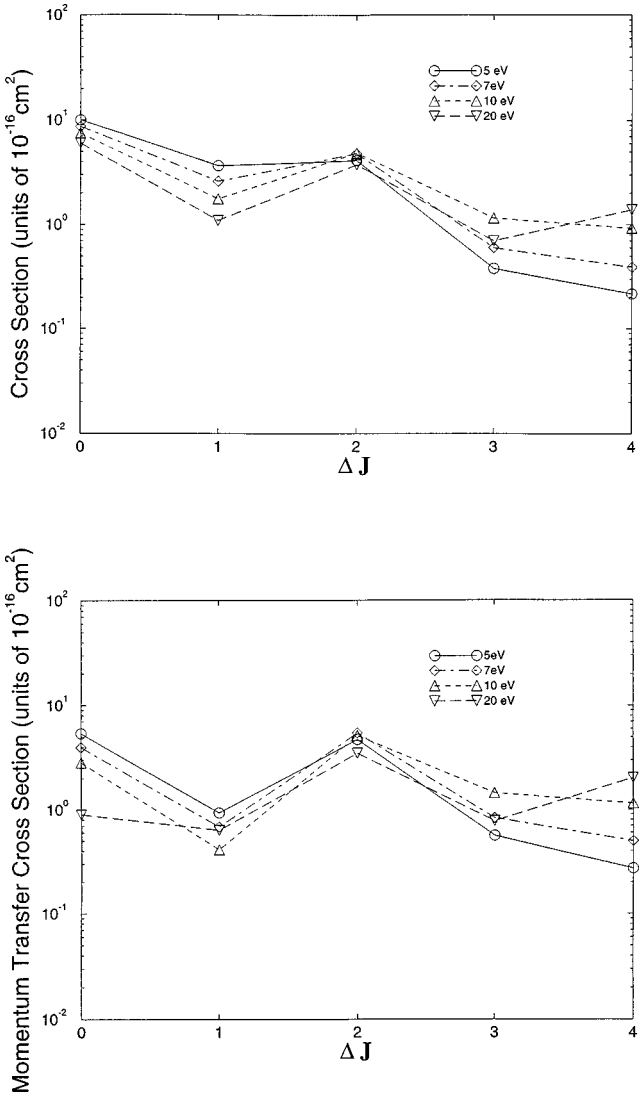

FIG. 6. Partial integral cross sections (top) and momentum-transfer cross sections (bottom) shown at three different collision energies and computed here as a function of the ΔJ values for the asymmetric rotor.

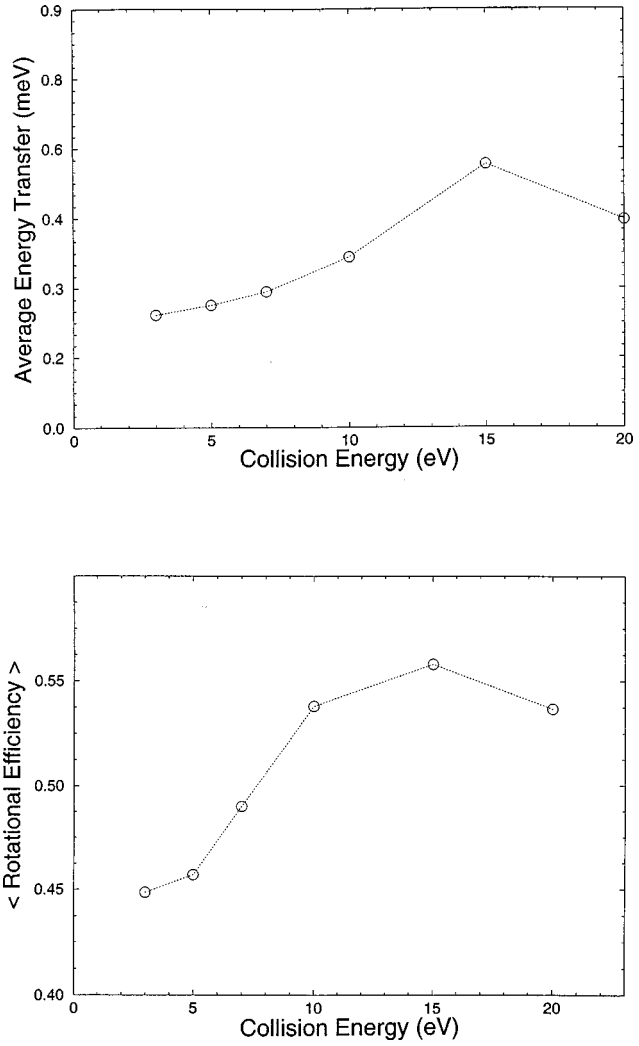

FIG. 7. Values of the average energy transfer in units of meV (top) and the rotational efficiency as a percentage value of the total flux (bottom) computed from the present rotationally inelastic transitions.

fairly small value of the permanent dipole moment (0.21 a.u.) we see that the elastic process remains the most probable at all collision energies, at variance with what has been found earlier by our calculations for the SO_2 [37] and H_2O [38] polar molecules, both of which exhibit larger permanent dipole moment values.

We also see from the results shown in Fig. 5 that the permanent molecular quadrupole plays an important role in this case since both its components, the one along the z axis and the asymmetric component $(\Theta_{xx}-\Theta_{yy})$, are larger than that from the dipole moment [31]. As the latter quantity could be taken to be chiefly responsible for the $\Delta J=2$ transitions at low energies, we verify here that the inelastic process for the $0\rightarrow 2$ transitions (open triangles) yields larger cross section than the one for the dipole transition (open squares): The latter dominates at low energies, while the former becomes markedly larger as $E_{\rm coll}$ increases. We also see from the figure that the $\Delta J=3$ and 4 excitations from the $J=0$ level are also rather sizable and exhibit a marked increase from 5 to 10 eV. On the whole, in fact, all the inelastic cross sections for exciting a ''cold'' ozone molecule are found to be rather large, especially as the collision energy reaches the 10-eV threshold value.

The corresponding behavior of the state-to-state inelastic cross sections, as a function of energy and ΔJ values, is shown in Fig. 6, where we report the partial integral cross sections (top) and the partial momentum transfer cross sections (bottom) at several collision energies and as a function of ΔJ.

It is interesting to note that the elastic cross sections dominate the low-energy regime, while inelasticity becomes larger as energy increases. Furthermore, in spite of the modest value of the dipole moment, the $\Delta J=1$ transitions have fairly large cross sections but, as mentioned before, the quadrupole-dominated $\Delta J=2$ transitions are still larger and appear to be the largest inelastic cross sections.

To further analyze the overall efficiency of the rotational excitation process of low-energy electrons with ozone molecules, it is of interest to evaluate the following quantities. The first is called the average energy transfer $\langle \Delta E_{\rm rot}\rangle$ from a given initial level $J=0$,

$$\langle \Delta E_{\rm rot} \rangle_{|J\tau\rangle=0} = \frac{\Sigma_{|J\tau\rangle\neq 0} \sigma_{0\to|J\tau\rangle} \Delta\varepsilon_{|J\tau\rangle}}{\sigma_{\rm tot}}, \tag{33}$$

a function of collision energy. Here $\Delta\varepsilon$ represents the energy spacings between rotational levels, given in meV. A further quantity could be obtained by defining the rotational efficiency as given by

$$P_{\rm rot}[|J\tau\rangle=0|E] = \frac{\Sigma_{|J\tau\rangle\neq 0} \sigma_{0\to|J\tau\rangle}}{\sigma_{\rm tot}}, \tag{34}$$

which therefore compares the relative flux going into excited states with the one going into the elastic channel. It is therefore a dimensionless probability function from a given initial rotational state of the molecule. Here $\sigma_{\rm tot}=\Sigma\sigma_{0\to|J\tau\rangle}$.

The results of the present calculations are shown in Fig. 7, where the upper part reports the behavior of $\langle \Delta E_{\rm rot} \rangle_{|J\tau\rangle=0}$ over the range of energies we have examined in the present work. Due to the fairly narrow spacings between rotational levels in ozone, we see that the amount of energy being transferred is rather small, a feature that seems to suggest that electrons do not efficiently ''heat'' ozone into excited rotational levels. In fact, the efficiency of the process is rather high, as one can gather from the behavior of $P_{\rm rot}(|J\tau\rangle=0|E)$ reported in the lower part of the same figure. We see there, in fact, that, over the examined range of energies the excitation efficiency goes from 45% up to 55%, indicating that about half of the overall flux goes into exciting the rotational channels (a result obtained within a FN approximation approach, which still decouples the vibrational channels). It is also interesting to note that both quantities show a maximum around 16 eV, which is near the energy region ($\sim$18 eV) where earlier calculations [17] suggested the possible presence of shape resonances of A_1 and B_2 symmetry from an ESE treatment of the interaction. Given the fact that in our computations we have also included polarization forces, it is not surprising to find the maximum shifted to lower energies. The more recent ESE calculations [18] suggest the two resonances to be at about 11 eV (A_1) and 14 eV (B_2), respectively, while the experiments [12] see such resonances in the inelastic channels only, as we discussed before. In any event, the analysis of such low-energy resonances is outside the scope of the present work and requires a more specific and detailed study of computed eigenphase sums in each contributing IR in order to be properly answered. We are currently addressing this point with an additional set of calculations [34].

V. CONCLUSIONS

In the present work we have carried out full quantum calculations for the low-energy scattering of electrons from the O_3 molecule in its ground electronic state and we have considered it as being fixed at its equilibrium geometry. The aim of this work was to verify the importance of dipole scattering in this system and the capability of our nonempirical model to describe the observed angular distributions of the electrons for elastic and rotationally inelastic channels. The coupled equations solved within our SCE approach to the electron scattering dynamics thus appear to realistically reproduce the experimental findings.

As we had found out with previous examples of polar molecules [37,38], the comparison with available DCSs provides a much more reliable and stringent test of the quality of a theoretical method. In the present case, therefore, we have compared our computed elastic (rotationally summed) DCSs at several energies with the available experiments [5,12] and found them to be in very good agreement with the measured data over a region of energy values from 3 to 20 eV.

ACKNOWLEDGMENTS

The financial support of both the Italian National Research Council (CNR) and the Italian Ministry for University and Research (MURST) is gratefully acknowledged. We are grateful to Professor M. T. Lee for having sent us his computed values for the cross sections prior to publication and to Professor Marco Lima and M. H. F. Bettega for sending us their pseudopotential results, which are still unpublished. We also wish to thank Dr. N. J. Mason for sending us his unpublished elastic cross section measurements.

[1] R. P. Wayne, in *Handbook of Environmental Chemistry*, edited by O. Hunzinger (Springer-Verlag, Berlin, 1989), Vol. 2, Pt. E.
[2] K. Yoshino, D. E. Freeman, J. R. Esmond, and W. H. Parkinson, Planet. Space Sci. **36**, 395 (1988).
[3] R. J. Celotta, S. R. Mielczarek, and C. E. Kuygatt, Chem. Phys. Lett. **24**, 428 (1974).
[4] N. Swanson and R. J. Celotta, Phys. Rev. Lett. **35**, 783 (1975).
[5] T. W. Shyn and C. J. Sweeny, Phys. Rev. A **47**, 2919 (1993).
[6] W. M. Johnstone, N. J. Mason, W. R. Newell, P. Biggs, G. Marston, and R. P. Wayne, J. Phys. B **25**, 3873 (1992).
[7] J. A. Davies, W. M. Johnstone, N. J. Mason, P. Biggs, and R. P. Wayne, J. Phys. B **26**, L767 (1993).
[8] N. J. Mason, J. M. Gingell, J. A. Davies, H. Zhao, I. C. Walker, and M. R. F. Siggel, J. Phys. B **29**, 3075 (1996).
[9] K. A. Newson, M. S. Luc, S. D. Prince, and N. J. Mason, Int. J. Mass Spectrom. Ion Processes **148**, 203 (1995).
[10] I. C. Walker, J. M. Gingell, N. J. Mason, and G. Marston, J. Phys. B **29**, 4749 (1996).
[11] J. D. Skalny, S. Matejcik, A. Kiendler, A. Stamatovic, and T. D. Märk, Chem. Phys. Lett. **225**, 112 (1996).
[12] M. Allan, K. R. Asmis, D. B. Popovic, M. Stepanovic, N. J. Mason, and J. A. Davies, J. Phys. B **29**, 4727 (1996).
[13] A. Banichevich and S. D. Peyerimhoff, Chem. Phys. **174**, 93 (1993).
[14] K. N. Joshipura, Pramana, J. Phys. **32**, 139 (1989).
[15] K. N. Joshipura and M. P. Patel, Pramana, J. Phys. **39**, 293 (1992).
[16] Y. Okamoto and Y. Itikawa, Chem. Phys. Lett. **203**, 61 (1993).
[17] B. K. Sarpal, K. Pfingst, B. M. Nestmann, and S. D. Peyerimhoff, Chem. Phys. Lett. **230**, 231 (1994).
[18] M. T. Lee, S. R. Michelin, T. Kroin, and L. E. Machado, J. Phys. B **31**, 1781 (1998).
[19] F. A. Gianturco and A. K. Jain, Phys. Rep. **143**, 347 (1986).

[20] F. A. Gianturco, J. A. Rodriguez-Ruiz, and A. K. Jain, Phys. Rev. A **48**, 4321 (1993).
[21] See, e.g., F. A. Gianturco, D. G. Thompson, and A. K. Jain, in *Computational Methods for Electron-Molecule Collisions*, edited by W. M. Huo and F. A. Gianturco (Plenum, New York, 1994).
[22] P. G. Burke, N. Chandra, and F. A. Gianturco, J. Phys. B **5**, 2212 (1971).
[23] U. Fano and D. Dill, Phys. Rev. A **6**, 185 (1972).
[24] O. H. Crawford and A. Dalgarno, J. Phys. B **4**, 494 (1971).
[25] I. Itikawa, Phys. Rev. **46**, 117 (1976).
[26] C. W. Clark, Phys. Rev. A **16**, 1419 (1977).
[27] D. W. Norcross and N. T. Padial, Phys. Rev. A **25**, 226 (1982).
[28] D. W. Norcross, Phys. Rev. A **25**, 764 (1982).
[29] F. A. Gianturco, J. Phys. B **24**, 3837 (1991).
[30] M. J. Prisch, G. W. Trucks, H. B. Schlegel, P. M. W. Gill, B. G. Johnson, M. A. Robb, J. R. Cheeseman, T. Keith, G. A. Petersson, J. A. Montgomery, K. Raghavachari, M. A. Al-Laham, V. G. Zakrewski, J. V. Ortiz, J. B. Foresman, C. Y. Peng, P. Y. Ayala, W. Cheng, M. W. Wong, J. L. Andres, E. S. Replogle, R. Ganperts, R. L. Martin, D. J. Fox, J. S. Binnkley, D. J. Defrees, J. Baker, J. P. Steward, M. Head-Gordon, C. Gonzalez, and J. A. Pople, GAUSSIAN 94, Revision B.2, Gaussian Inc., Pittsburgh, PA, 1995.
[31] K. M. Mack and J. S. Muenter, J. Chem. Phys. **66**, 5278 (1977).
[32] N. J. Mason (private communication).
[33] S. Althorpe, F. A. Gianturco, and N. Sanna, J. Phys. B **28**, 4165 (1995).
[34] F. A. Gianturco, R. R. Lucchese, R. Curik, and N. Sanna (unpublished).
[35] For an extensive discussion of this point see F. A. Gianturco and P. Paioletti, in *Frontiers in Electronic-Scattering*, edited by K. Beker (Kluwer, Amsterdam, 1998).
[36] M. A. P. Lima and M. H. F. Bettega (private communication).
[37] F. A. Gianturco, P. Paioletti, and N. Sanna, J. Phys. B **30**, 4535 (1997).
[38] F. A. Gianturco, P. Paioletti, S. Meloni, N. Sanna, and R. R. Lucchese, J. Chem. Phys. **108**, 4002 (1998).